ResearchGate

See discussions, stats, and author profiles for this publication at: https://www.researchgate.net/publication/7049412

The effect of manganese(II) on the structure of DNA/HMGB1/H1 complexes: Electronic and vibrational circular dichroism studies

ARTICLE *in* BIOPOLYMERS · OCTOBER 2006

Impact Factor: 2.39 · DOI: 10.1002/bip.20544 · Source: PubMed

CITATIONS
15

READS
18

5 AUTHORS, INCLUDING:

A. M. Polyanichko
Saint Petersburg State University
31 PUBLICATIONS **218** CITATIONS
SEE PROFILE

Elena Vsevolodovna Chikhirzhina
Russian Academy of Sciences
33 PUBLICATIONS **218** CITATIONS
SEE PROFILE

Valery Andrushchenko
Academy of Sciences of the Czech Republic
56 PUBLICATIONS **899** CITATIONS
SEE PROFILE

Available from: Valery Andrushchenko
Retrieved on: 26 January 2016

A. M. Polyanichko[1,2]
E. V. Chikhirzhina[3]
V. V. Andrushchenko[1]
V. I. Vorob'ev[3]
H. Wieser[1]
[1] *Department of Chemistry, University of Calgary, Calgary, Canada*

[2] *Department of Physics, St. Petersburg State University, St. Petersburg, Russian Federation*

[3] *Institute of Cytology of the Russian Academy of Sciences, St. Petersburg, Russian Federation*

The Effect of Manganese(II) on the Structure of DNA/HMGB1/H1 Complexes: Electronic and Vibrational Circular Dichroism Studies

Received 13 April 2006; revised 22 May 2006; accepted 22 May 2006
Published online 26 May 2006 in Wiley InterScience (www.interscience.wiley.com). DOI 10.1002/bip.20544

Abstract: *The interactions were studied of DNA with the nonhistone chromatin protein HMGB1 and histone H1 in the presence of manganese(II) ions at different protein to DNA and manganese to DNA phosphate ratios by using absorption and optical activity spectroscopy in the electronic [ultraviolet (UV) and electronic circular dichroism ECD)] and vibrational [infrared (IR) and vibrational circular dichroism (VCD)] regions. In the presence of Mn^{2+}, the protein–DNA interactions differ from those without the ions and cause prominent DNA compaction and formation of large intermolecular complexes. At the same time, the presence of HMGB1 and H1 also changed the mode of interaction of Mn^{2+} with DNA, which now takes place mostly in the major groove of DNA involving N_7(G), whereas interactions between Mn^{2+} and DNA phosphate groups are weakened by histone molecules. Considerable interactions were also detected of Mn^{2+} ions with aspartic and glutamic amino acid residues of the proteins.* © 2006 Wiley Periodicals, Inc. Biopolymers 83: 182–192, 2006

This article was originally published online as an accepted preprint. The "Published Online" date corresponds to the preprint version. You can request a copy of the preprint by emailing the Biopolymers editorial office at biopolymers@wiley.com

Keywords: *DNA–protein interactions; circular dichroism; infrared/vibrational circular dichroism spectroscopy, HMGB1; histone H1*

Correspondence to: A. M. Polyanichko; e-mail: ampolyan@ucalgary.ca

Contract grant sponsor: Natural Sciences and Engineering Research Council of Canada, Alberta Heritage Foundation for Medical Research (AHFMR), and the Russian Foundation for Basic Research (RFBR), the Federal Agency of Science and Innovation, Program "Leading Scientific Schools of Russia", and The Government of St. Petersburg.

Contract grant number: 04-04-49429, 05-04-49217 (RFBR), 02.445.11.7338, 9396.2006.4, and PD06-1.4-55.

Biopolymers, Vol. 83, 182–192 (2006)

© 2006 Wiley Periodicals, Inc.

INTRODUCTION

Metal ions play essential roles in about one-third of the enzymes.[1–3] They are also known to be important cofactors not only for enzymes but also for proteins performing transport and structural functions. Manganese ions are not the exception.[4] Different enzymes and regulatory proteins require Mn^{2+} to function properly in the living cell.[5–11] Many of these proteins interact directly with DNA and it is important to understand not only the interaction mechanisms but also the role the ions play in forming the DNA–protein complexes. In some instances, the activity of manganese-dependent systems is modulated by other nuclear proteins normally not involved. Mn^{2+} ions were reported to be essential cofactors for the proper functioning of the systems, which recruit HMGB-domain proteins. One of the interesting examples is the participation of High Mobility Group 1 and 2 (HMGB1/2) nonhistone proteins, formerly called HMG1/2,[12] in the functioning of proteins encoded by Recombination Activation Genes (RAG1/RAG2) during recombination events.[13–16] HMGB proteins constitute the family of chromatin proteins that contain the HMG-Box structural motif (HMGB domain). The abundant members of this family are well known for their unusual DNA binding properties, which are characteristic for the motif.[17,18] It was shown earlier that these proteins are able to recognize a variety of structural distortions in the DNA double helix as well as unusual DNA structures such as Holliday junctions[19,20] and DNA cruciforms.[21,22] HMGB proteins can also induce bends in DNA up to 140°.[17,23] Although these proteins were assigned mostly structural functions, their specific role remains unclear. To reflect these functions they were also called architectural factors of chromatin.[24,25] In some cases, they act together with other proteins as part of rather large DNA–protein complexes.[18,23,26–33] Protein–protein interactions affect many DNA binding properties of HMGB1, especially in complex DNA–protein systems.[34–36] It was shown recently that HMGB proteins modulate some recombination events.[13–16]

Histone H1 is one of the most studied chromatin proteins.[37–40] It binds to a linker DNA at the entrance and exit of the nucleosome. This interaction takes place through the major groove of DNA, bending it around the protein. It is therefore quite different from the interaction of HMGB1 with DNA. In fact, several attempts were made to study their mutual influence on DNA binding.[26–28] The results of these studies suggest that these two proteins act cooperatively rather than competitively in binding DNA. The purpose of our present study is to investigate complexes of DNA–Mn^{2+}–HMGB/H1 based on the structural information provided by the combination of electronic absorption [ultraviolet (UV)] and electronic circular dichroism (ECD) as well as vibrational absorption [infrared (IR)] and vibrational circular dichroism (VCD). The combination of electronic and vibrational spectroscopies provide complementary information about the systems and becomes especially important when dealing with large DNA–protein complexes. The main challenge for studying such systems in the UV range is a significant contribution of light scattering, which leads to the formation of characteristic nonconservative spectral pattern, called ψ-type CD spectra (PSI: Polymer and Salt Induced), which look similar to each other for all scattering systems. This type of spectra was first assigned to a PSI or ψ form of DNA,[41] but was later attributed to electrostatic condensation/aggregation of DNA in the presence of another polymer and at high concentration of counterions. In most cases, large DNA–polymer complexes cause considerable light scattering, which does not allow one to make judgments about conformational changes in the molecules directly by the shape of ECD spectra.[42] This limitation allows one to use only dilute, or true, polymer solutions in CD experiments. However, functioning of DNA in living cells requires the formation of large supramolecular complexes, which are closer to aggregates than to molecular solutions.

Infrared spectroscopic methods, i.e., absorption (IR) and VCD, contain more structural information about the system, because there are many vibrational modes in each molecule that manifest themselves in the spectra as a number of well-resolved bands. Moreover, as the wavelength of IR radiation is longer, compared to UV, one can also study large complexes without significant contributions of light scattering.[43] VCD is a relatively new tool for investigating the structure of biological macromolecules.[44–46] It is very sensitive to structural changes in the macromolecules and considerably more informative for structural analysis compared to ECD. For example, the analysis of VCD spectra yields information about the mutual orientation of the different chemical groups within a molecule as well as their participation in interactions with other molecules or ions. This information is provided by vibrations of different chemical groups, which can be distinguished in absorption (IR) and VCD spectra as characteristic bands.

MATERIALS AND METHODS

To form DNA–protein complexes, histone H1 (MW 21,000) and nonhistone chromatin protein HMGB1 (MW

26,500) were isolated from the nuclei of calf thymus. The former was extracted with 5% perchloric acid followed by precipitation with 3 volumes of acidic acetone at −20°C as described by Oliver et al.,[47] and HMGB1 was isolated according to the method of Johns.[48] The purity of the products was tested with sodium dodecyl sulfate–polyacrylamide gel electrophoresis (SDS-PAGE).[49] The protein concentration was determined by UV absorbance using extinction coefficients $\varepsilon_{230} = 41{,}000M^{-1}$ cm^{-1} (H1) and $\varepsilon_{280} = 33{,}000M^{-1}$ cm^{-1} (HMGB1).[28]

Solutions of calf thymus DNA (Sigma-Aldrich, Oakville, ON, Canada) were sonicated at 0°C (ice chilled) for a total of 5 min. The molecular weight of the DNA samples was checked by agarose gel electrophoresis. The distribution of the lengths of the fragments determined by scanning the gel pattern peaked at ∼550 base pairs.

All inorganic salts were spectroscopic grade (Alfa Aesar, Ward Hill, MA, USA) except sodium cacodylate, which was 98% Sigma Ultra grade (Sigma-Aldrich, USA). All aqueous solutions were prepared in double-distilled deionized water. Deuterium oxide (99.9% D_2O) for measuring the IR and VCD spectra was purchased from Sigma-Aldrich (Oakville, ON, Canada).

The w/w ratio of HMGB1 to H1 was 1:3 (0.42 molar ratio) for all systems. The w/w ratio r of protein (total of HMGB1 and H1) to DNA was used as the variable for all measurements. DNA–protein complexes were obtained by direct mixing of comparable volumes of DNA and protein stock solutions. Systems with protein to DNA ratio were investigated in the $0.008 \leq r \leq 3.3$ range.

UV Spectroscopy

Mn^{2+}–DNA–protein complexes were obtained by direct mixing of either DNA–Mn^{2+} with manganese-free protein, or mixing manganese-free DNA with protein–Mn^{2+} solutions. To investigate the complexes in a possibly broader r range, avoiding intensive aggregation in the solution, moderate sample concentrations should be used. To achieve this goal, the whole r range under investigation was divided into two subregions below and above $r = 0.085$. Complexes with $r < 0.085$ were prepared with DNA concentration equal to 300 μg/mL, while complexes with $r > 0.085$ were prepared with protein concentration equal to 23 μg/mL. This approach allowed us to significantly reduce DNA concentration in the complexes with higher r, and keeping the protein concentration below 25 μg/mL. The samples were incubated at room temperature for at least 20 min before measuring. All complexes were prepared in solutions of 15 mM NaCl at neutral pH. The [Mn]/[P] molar ratio R, where [Mn] and [P] are the molar concentrations of manganese ions and DNA phosphates, respectively, ranged from 0.006 to 180 (0.005–10.0 mM $MnCl_2$ absolute). The concentration of DNA was varied between 7 μg/mL (at $r = 3.3$) and 300 μg/mL (at $r = 0.008$).

The UV and ECD spectra were recorded with a Jasco-715 spectropolarimeter (Jasco Corp., Japan) in 1-mm quartz cells and are reported below as the averages of three sequential scans between 190 and 320 nm using the standard Jasco software.

Infrared Spectroscopy

Solutions for IR and VCD were prepared in $10^{-2}M$ cacodylate buffer (pH 6.5 ± 0.5). The protein to DNA ratio was kept at $r = 0.1$ for all complexes, which is close to their physiological content in chromatin. DNA–protein complexes were prepared in dilute aqueous solutions mixing equal volumes of DNA and the protein components containing Mn^{2+} in appropriate concentrations. Complete deuterium exchange and target sample concentrations were achieved by lyophilizing and redissolving all solutions three times in appropriate amounts of D_2O. Samples were contained in a demountable cell (International Crystal Laboratories, Garfield, NJ) composed of two BaF_2 windows separated by a 50-μm Teflon spacer. Samples (30 μL) were deposited directly on one of the cell windows and then covered with the second window. The final concentration of DNA in the sample was 40 mg/mL ([P] = 0.13M). Mn^{2+} ion concentration was varied between 0 and 1.3M (0–10 [Mn]/[P]). The temperature of the cell was monitored at 23 ± 0.5°C with a copper-constantan thermocouple (Omega Engineering, Inc., Stamford, CT, USA).

The IR and VCD spectra were measured simultaneously between 1800 and 750 cm^{-1} with the VCD instrument described elsewhere.[50] A total of 7500 ac scans was accumulated (85 min scan time) and ratioed against 500 dc scans for the VCD spectra, and 500 dc scans were accumulated for the absorption spectra, all at 8 cm^{-1} resolution. Each system (R, r) was measured at least three times at equal conditions and averaged. These data were used further to estimate a noise level in the VCD spectra. The VCD spectra were corrected for polarization artefacts by subtracting the spectra of the solvent obtained at the same conditions. The absorption and VCD spectra were interpolated with a factor 8 according to the 4-point cubic spline algorithm supplied with the Lab Calc package.[51]

RESULTS

UV Experiment

UV and ECD spectra were recorded for different protein to DNA ratios (r) at different concentrations of manganese ions ($0.1 \leq R \leq 11$). Typical ECD spectra of the complexes with 0.1 and 6.0 mM $MnCl_2$ (R = 0.1 and 6.6, respectively) are plotted in Figures 1 and 2. Below 0.1 mM Mn^{2+}, the ECD spectra of the DNA–protein complexes were not affected, indicating no spectroscopically noticeable structural changes in the complexes (data not shown). For complexes with r values between 0.008 and 0.08 and in the presence of 0.1 mM $MnCl_2$ ($R = 0.1$) appreciable spectral changes occurred only in the region between 200 and

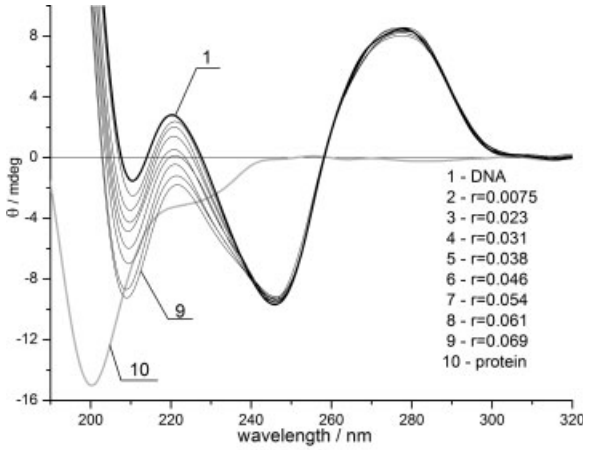

FIGURE 1 ECD spectra of complexes with different protein to DNA ratios r at 0.1 mM $MnCl_2$ ($R = 0.1$). (a) 300 μg/mL DNA ($R = 0.1$): 1, DNA ($r = 0$); 2, $r = 0.0075$; 3, $r = 0.023$; 4, $r = 0.031$; 5, $r = 0.038$; 6, $r = 0.046$; 7, $r = 0.054$; 8, $r = 0.061$; 9, $r = 0.069$; 10, proteins only (23 μg/mL). (b) 1, DNA ($r = R = 0$); 2, $r = 0.0075$; 3, $r = 0.15$; 4, $r = 0.19$; 5, $r = 0.41$; 6, $r = 0.68$; 7, proteins.

240 nm for which the negative ECD intensity increased gradually with the protein to DNA ratio (Figure 1a) due to the increasing protein contribution similar to the systems without manganese.[52] At higher protein to DNA ratios, significant Mn^{2+}-induced changes occur in the ECD of the DNA–protein complexes between 260 and 300 nm (Figure 1b).

For the complexes with $0.09 < r < 0.15$ (Figure 1b), the maximum of the positive DNA band shifts from 275 to 285 nm and decreases in intensity. CD of the systems with higher r appears as ψ-type CD spectra, indicating the presence of supramolecular complexes in this r interval. All the ψ spectra are observed on either side of $r \sim 0.4$. Near $r = 0.4$ (Figure 1b, curve 5), light scattering becomes so intense that almost no ECD signal can be seen in this opaque r region, which becomes wider with increasing Mn^{2+} concentration and at 0.8 mM Mn^{2+} it covers the whole interval of $0.26 < r < 0.41$ (Figure 3). Contributions from the ψ-type spectra and light scattering obscure possible spectral changes, which might occur as a result of modifications in DNA secondary structure.

In the solutions with 0.8 mM Mn^{2+} ($R = 0.9$) at $r < 0.04$, the ECD spectra of the complexes are the same as those of DNA–Mn^{2+} alone.[52] A fast transition to the ψ-type ECD spectra begins at $r \sim 0.12$ and is completed by $r \sim 0.19$ (Figure 3). As mentioned above, DNA–protein interactions lead to a dramatic increase in light scattering at $0.26 < r < 0.41$. Upon further increasing the protein concentration ($0.41 < r < 1.0$) the UV spectra (data not shown) return to their normal shape, but there are still some signs of rather strong light scattering by the DNA–protein complexes. The corresponding ECD spectra can be attributed again to the ψ type. This behavior likely means that there may be two different modes of DNA–protein interactions within the investigated r range. This interpretation is confirmed by the considerably higher intensity at $r = 0.19$ than at $r = 0.68$ (Figure 3) and implies that the high turbidity of the solutions with the intermediate protein to DNA ratios (r) reflects a structural rearrangement of the complexes. The similar situation occurred for the complexes with 0.1 mM $MnCl_2$, whereas upon further increasing the protein content up to $r = 3.3$ in the presence of 0.8 mM Mn^{2+} or higher (spectra not

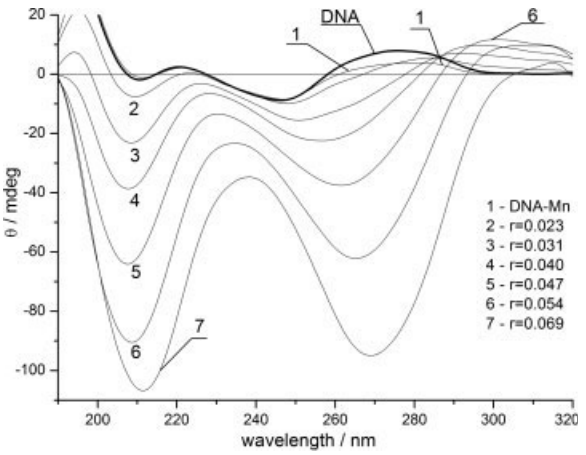

FIGURE 2 ECD spectra of complexes with different protein to DNA ratios r and in the presence of 6.0 mM $MnCl_2$ ($R = 6.6$): 1, DNA; 2, DNA–Mn^{2+}; 3, $r = 0.023$; 4, $r = 0.031$; 5, $r = 0.040$; 6, $r = 0.047$; 7, $r = 0.054$; 8, $r = 0.069$.

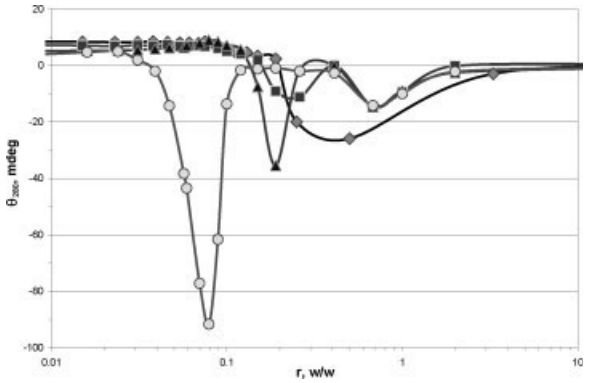

FIGURE 3 Dependence of DNA ellipticity at 280 nm (θ_{280}) on protein to DNA ratio r at different $MnCl_2$ concentrations ([Mn]/[P] ratios R): diamonds, 0.0 mM $MnCl_2$ ($R = 0$); squares, 0.1 mM $MnCl_2$ ($R = 0.1$); triangles, 0.8 mM $MnCl_2$ ($R = 0.9$); circles, 6.0 mM $MnCl_2$ ($R = 6.6$).

shown) the DNA–protein complexes did not precipitate. Thus, the addition of relatively small amounts of Mn^{2+} ions affected the aggregation processes considerably. Increasing the Mn^{2+} concentration to 6 mM ($R = 6.6$) (Figure 2) and further to 10 mM ($R = 11$) (not displayed) did not change the spectral pattern qualitatively but led to large quantitative shifts in terms of protein to DNA ratios (Figure 3). The dramatic increase in ECD intensity occurred between $0.024 < r < 0.08$ (Figure 2), whereas no ECD signal was detected between $0.1 < r < 0.4$ at this manganese concentration (Figure3) and the ψ spectra appeared at higher r. Precipitation of the complexes was not observed at high r. Noteworthy is that the spectral behavior of the systems does not depend on the sequence of the addition of individual components to the solution.

IR Experiment

The IR and VCD spectra of the DNA and proteins were recorded in the carbonyl (1750–1450 cm^{-1}) and in the sugar–phosphate regions (1150–750 cm^{-1}). IR[53–57] and VCD[58–64] band assignments for DNA and its constituents (nitrogen bases and sugar–phosphate backbone) have been extensively described in the literature. They are summarized in Table I based

Table I The Assignment of the Major Vibrations in Mn^{2+}–DNA–HMGB1/H1 Complex

Band Position in Unbound State (cm^{-1})		Band Position in Complex (cm^{-1})		
Absorption	VCD	Absorption	VCD	Proposed Assignment[b]
[a]	—	1730	1710(+)	C=O stretching vibration in Asp side chain
[a]	—	1715		C=O stretching vibration in Glu side chain
1690	1700(−)	1693	1698(−)/1688(+)	Stretching vibrations of C2=O in thymine
1682	—	1688, 1676	—	Superposition of 1688/1678 cm^{-1} peaks (unbound) and 1693/1678 cm^{-1} peaks (complex) corresponding to C=O groups in guanine and cytosine (see below)
1678	1666(+)	1678/1668	1662(+)	Stretching vibrations of C=O groups in guanine and cytosine in presence of proteins (1678) and both proteins and Mn^{2+} (1668)
1648	1648(+)	1644	—	C2=O stretching of cytosine and C4=O of thymine, C6=O of guanine, C=C of cytosine
1623	1638(+)	1623	1638(+)	Adenine, thymine ring vibrations
1572, 1560	—	1572, 1560	—	Superposition of purine ring vibrations, including C—ND_2 (1572 cm^{-1} and C=N (1560 cm^{-1})
1538, 1519, 1500	—		—	Cytosine ring vibrations
1502	1504(−)	1502	1504(−)	C=N stretching in cytosine
1086	1091(−)/1074(+)	1086	1091(−)/1074(+)	Symmetrical vibrations of O=P=O bonds
1053	1056(+)	1053	1056(+)	Stretching vibrations of C—O bonds in sugar ring
1021	1034(−)/1008(+)	1021	1034(−)/1008(+)	deoxyribose vibration
970	972(−)	970	972(−)	Sugar ring vibrations
938, 895, 836	936(−)/896(+)/—	938, 895, 836	936(−)/896(+)/—	Sugar ring vibrations; DNA B-form markers

[a] This vibration in the unbound state was poorly resolved and the precise position of the maximum was not determined.
[b] Assignments are based on Refs. 46, 52, and 65.

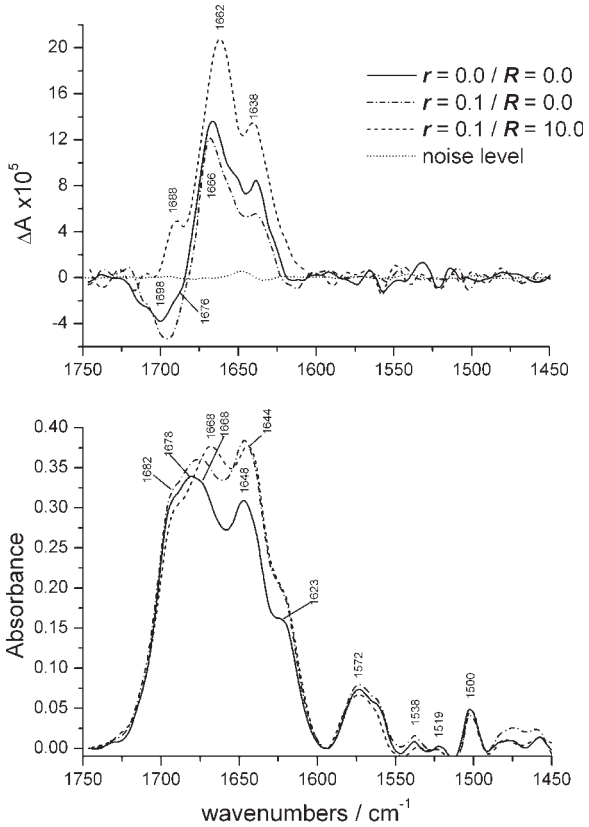

FIGURE 4 IR (bottom) and VCD (top) spectra in carbonyl region of DNA–protein complexes with protein to DNA ratio $r = 0.1$ (w/w) at key [Mn]/[P] ratios (R). Solid, DNA ($r = 0$ and $R = 0.0$); dash-dot, $r = 0.1$ and $R = 0.0$; dash, $r = 0.1$ and $R = 10$; dot, noise estimation for VCD measurement.

on a recent review[46] and two analyses of DNA interacting with manganese ions.[52,65]

Carbonyl Region. Most of the absorption and VCD features of DNA ($r = R = 0.0$) between 1750 and 1450 cm^{-1} (Figure 4) originate from C=O stretching and skeletal ring vibrations of the nitrogenous bases.

VCD features especially for nucleic acids appear often as ''couplets'' with positive/negative or negative/positive lobes centered at the wavenumber position of a corresponding absorption. The couplets arise from coupled vibrations of identical oscillators in a helical arrangement and are therefore diagnostic of the mutual proximity and relative geometry of the bases.

The IR and VCD spectra of DNA alone and of both HMGB/H1 protein complexes alone have been described in details elsewhere.[43,52] The IR and VCD spectra of the DNA and DNA–HMGB1/H1 complex in the region 1750–1450 cm^{-1} are shown in Figure 4. The absorption spectrum of the DNA–protein complex at $r = 0.1$ and $R = 0.0$, while generally similar to that of DNA alone, shows an increased intensity of the main composite band, which also contains an absorption from the proteins in the amide I region[62,66] at $\sim$1645 cm^{-1} and contributes to the intensity of the 1648-cm^{-1} DNA band. The contributions from the amide I and II modes can be considered constant for all complexes due to the negligible spectral changes of these bands compared to changes in the spectra of DNA achieved by the tenfold excess of DNA over proteins in the complexes. Simultaneously, the contour of the composite absorption band at 1678 cm^{-1} with its shoulder at 1668 cm^{-1} changed, revealing a lower intensity of the former and greater intensity of the latter. Upon addition of the manganese ions ($r = 0.1$, $R = 10$) a peak at 1678 cm^{-1} replaced the unresolved 1678/1668 cm^{-1} pair, while the 1648 cm^{-1} absorption shifted to 1644 cm^{-1} with nearly the same intensity.

The above changes in the spectra of DNA occur against the minute background intensity of the C=O stretching vibrations of aspartic (Asp) and glutamic (Glu) amino acid residues[67] in HMGB1 at 1730 and 1715 cm^{-1} (Figure 4). A corresponding weak VCD maximum emerges at 1710 cm^{-1} and appears to become more pronounced upon the addition of manganese. Noticeable changes in the VCD spectra of DNA in response to additions of the proteins and Mn^{2+} include the following. For the DNA–protein complex without Mn^{2+} ($r = 0.1$, $R = 0.0$), the negative lobe of the main feature at $\sim$1696 cm^{-1} has increased in intensity, whereas the intensity of the positive lobe has decreased with a slightly shifted maximum at 1666 cm^{-1}. Upon adding Mn^{2+} ($r = 0.1$, $R = 10$), the positive VCD lobe shifts to 1662 cm^{-1} and its intensity as well as that of the positive peak at 1638 cm^{-1} increased considerably. A similar shift in position and intensity increase were observed when only manganese ions with the same R ratio were added.[65] The difference between the DNA–protein complexes compared to the systems without the proteins is the positive lobe at 1688 cm^{-1}, which did not occur in the protein-free systems.[65]

Phosphate Region. Although no significant changes can be seen in the absorption spectra of the sugar–phosphate region of DNA upon addition of the proteins (Figure 5), addition of Mn^{2+} to the DNA–protein complex results in significant decrease of the symmetric PO_2^- band. A distinct shoulder appearing in the absorption spectrum of the DNA–protein complex at around 1108 cm^{-1} after addition of manganese ions might be attributed to the in-plane bending vibrations in Asp and Glu side chains.[67] Upon DNA interaction

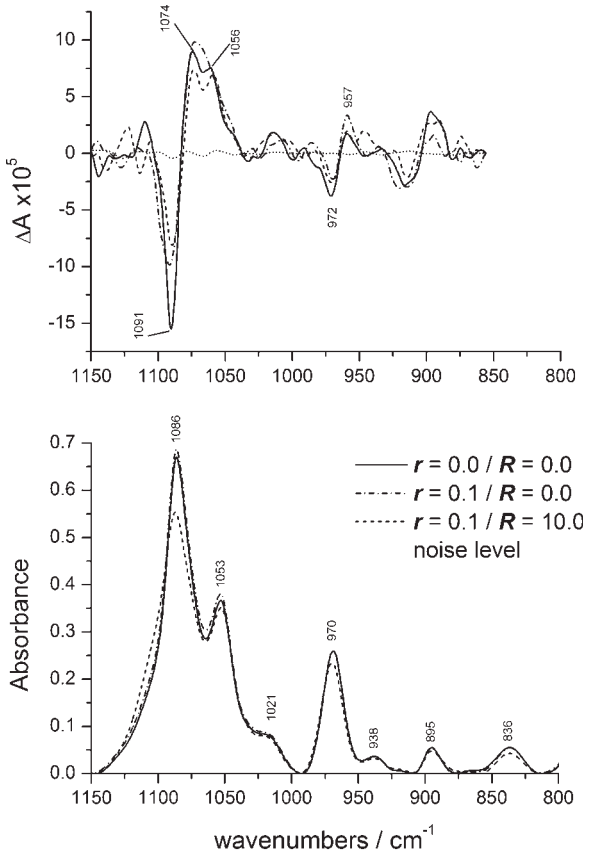

FIGURE 5 IR (bottom) and VCD (top) spectra in sugar–phosphate region of DNA–protein complexes with protein to DNA ratio $r = 0.1$ (w/w) at key [Mn]/[P] ratios (R). Solid, DNA ($r = 0$ and $R = 0.0$); dash-dot, $r = 0.1$ and $R = 0.0$; dash, $r = 0.1$ and $R = 10$; dot, noise estimation for VCD measurement.

with the protein only the negative VCD peak of the symmetric stretching mode of PO_2^- at 1086 cm^{-1} decreases in intensity, but both the negative and positive peaks of the 1091(−)/1074(+) cm^{-1} couplet in DNA diminish significantly upon adding Mn^{2+}.

DISCUSSION

The spectral behavior of the complexes in the UV region is different for the Mn^{2+}–DNA–protein complex than for the DNA–protein[36,43,68,69] and Mn^{2+}–DNA[52] complexes and depends on the protein to DNA ratio. The ECD spectra of the complexes indicate that several structural stages are occurring in the system, depending on the protein to DNA ratio (Figure 3), and supramolecular structures are formed during these stages. As observed previously, HMGB–DNA interactions lead to the formation of structurally different supramolecular complexes,[36,68] depending on the protein to DNA ratio. Some of these complexes were extremely sensitive to the protein content. The present systems are also very sensitive to the amount of Mn^{2+} added. At small Mn^{2+} concentrations ([Mn]/[P] ratio $R < 0.1$), DNA–protein complex formation is not noticeably affected by the metal ions. The increase in Mn^{2+} concentration in this interval promotes intermolecular interactions and the formation of supramolecular associations. At higher R, the spectra suggest that a structural rearrangement of the complexes occurs, which affects not only DNA–protein interactions but could also influence the DNA structure, causing the intensity increase of the ECD bands even though DNA remains in the B-form. The shift of the positive ECD maximum toward 280 nm and an appreciable change in its shape (Figure 1b, curve 3) reflects considerable changes in the electron structure of the bases. The changes are similar to those observed for the interaction of different ligands with N_7 atoms of guanine and adenine[52] located in the major groove. This process is accompanied by a strengthening of protein–protein interactions, which are much stronger now than in cases of binding the individual proteins to DNA. This is illustrated by the extensive aggregation of the complexes in solution. The formation of many scattering centers leads to the appearance of foggy solutions. At the same time, most of the complexes studied do not demonstrate the inclination to precipitate, which points to a certain degree of structural order rather than molecules associating with one another randomly. An important property of the system is that its components bind in equilibrium, which is also confirmed by the IR and VCD results.

A significant level of light scattering precludes observation of detailed structural properties of the complexes by UV spectroscopy. However, it is possible to obtain additional information by IR/VCD, since it enables one to study particles several orders of magnitude larger without considerable influence of light scattering.[43,61,62,70]

Without the proteins, the presence of Mn^{2+} leads to a significant intensity increase of almost all IR bands in the phosphate region,[52] which reflects the strong interaction of the metal ions with the sugar–phosphate backbone. Addition of the protein to DNA without the presence of Mn^{2+} produces no changes in the IR spectrum of DNA in this region (Figure 5). Yet, the presence of both proteins and Mn^{2+} together causes the decrease of the IR intensity of the symmetric PO_2^- stretching mode. The corresponding VCD couplet also decreases in intensity, which reflects the screening of the negative charges of the phosphate groups during the counterion binding. There is also a

slight increase in intensity of absorption at 1108 cm^{-1}, indicating possible participation of Aps and Glu amino acid residue side chains in the interaction with Mn^{2+} ions and DNA. Such an increase did not occur in the case of protein–Mn^{2+} or DNA–Mn^{2+} interactions alone and only occurs in the ternary system DNA–protein–Mn^{2+}, indicating that Mn^{2+} ions facilitate the DNA–Asp side chain interaction by screening PO_2^-. Simultaneously, the nearby sugar vibration mode remains unchanged in the VCD and IR spectra. The clearly separated phosphate and sugar VCD peaks at 1074 and 1056 cm^{-1}, respectively, are essentially equally intense in the spectra of ternary complex. The intensitiy and position of the sugar band are almost identical in all spectra, suggesting that the sugar does not participate in the interaction. This differs from the DNA–Mn^{2+} interaction without the proteins when not only IR but also VCD of this particular peak increased significantly.[52] The slight changes in the intensity of DNA IR band at 836 cm^{-1} (Figure 5) indicates that the presence of manganese ions facilitates changes in DNA geometry caused by HMGB1 binding. The sugars are exposed to the minor groove and in the presence of HMGB1 are likely inaccessible for the Mn^{2+} ions because the groove is occupied by the protein. In this case, it is also possible to explain the absence of strong interaction between the metal ions and the phosphate groups in terms of the proteins' influence. It was shown earlier that the C-terminal part of HMGB1, represented by the sequence of 30 dicarboxylic amino acid residues, is responsible for altering the tendency of the proteins to bind to DNA.[36,71] Possessing a high negative net charge, this tail of the protein likely interacts with the sugar–phosphate backbone, which is also negatively charged, inducing rather strong repulsive forces. This possibility is confirmed by the changes in the C=O stretching vibrations of Asp and Glu side chains. Increasing intensity of the corresponding bands in the absorption spectra indicate interaction of COO^- groups with the manganese counterions, while changes in VCD spectra at 1710 cm^{-1} reflect structural rearrangements of the protein tail. Considering that the concentration of the protein in the complex is small, the appearance of these features especially in VCD means appreciable interactions between manganese ions and the side chains of Asp and Glu amino acid residues.[43] Hence, the presence of the tail in the vicinity of the DNA might lead to a redistribution of the metal ions in the DNA hydration layers and their migration to the cloud of counter ions around the proteins' tail.

The IR spectral changes in the carbonyl region of the bases are more informative (Figure 4). The spectrum of the DNA–protein complex changes relatively little compared to DNA alone. The main difference is the increased intensity and shift of the peak at 1682 cm^{-1}, which likely results from the distortions of the double helix upon the interaction and the decrease of the distances between certain bases in the major groove. This observation is also supported by a slight decrease of the VCD signal reflecting stacking distortions. The addition of the manganese ions to the complex leads to several noticeable changes. The absorbance of the C=O stretch of guanine and cytosine at 1678 cm^{-1} increases in intensity, while C2=O vibration of thymine at 1693 shows no noticeable change. These carbonyls differ in their participation in hydrogen bonding—namely, the carbonyls of the guanines and cytosines participate in the base pairing, whereas C2=O groups of the thymines do not form hydrogen bonds with adenines and are exposed to the minor groove. Such changes in the vibrational modes of C=O groups of the bases are normally the result of distortions of the electron structure of the bases and usually occur upon the interaction of some ligands with N_7(G).[57] This interaction causes redistribution of the electron density of guanine ring directly affecting the vibrations of guanine's C=O groups and those of cytosine through the hydrogen bonds between the bases, while there is not much influence on the C2=O mode of thymine even if N_7(A) participates in similar interactions. This result confirms the UV data, which indicate that the manganese ions are involved in a rather strong interaction with the bases in the DNA major groove. According to our earlier study of DNA–HMGB1/H1 complexes[43] when both proteins are present in solution, histone H1 mostly interacts with DNA phosphates and the C-terminal domains of the HMGB1 molecules, leaving the major groove of DNA unoccupied. Although the geometry of the major groove is likely distorted due to the binding of HMGB1 and not enough space is left for histone H1 binding, it is still large enough to accommodate the metal ions. Moreover, narrowing of the major groove could facilitate simultaneous coordination of the Mn^{2+} ions to N_7(G) and oxygen atoms of phosphate groups.

The possibility of manganese interacting with the bases was already demonstrated for Mn^{2+}–DNA systems.[52] In that case, the picture was more complicated and coordination of manganese ions to the bases was observed in both DNA grooves. However, the interactions in the minor groove started only at high manganese to phosphate ratios after coordination of Mn^{2+} to N_7 of guanine in the major groove. In the present situation, no interaction of the metal ions with the bases in the minor groove could be observed in the presence of the proteins. This leads to the con-

clusion that the interactions in the minor groove are blocked by the proteins bound to DNA. The positive VCD peak at 1662 cm^{-1} attributed to C=O stretching of guanine and cytosine[52] almost doubled in intensity, indicating that the interaction is accompanied by significant redistribution of the electron density of the bases, which is also observed in the ECD spectra (Figures 1 and 2).

The presence of HMGB1 also affects the vibrational mode of the carbonyls in the minor groove, as revealed by the changes in VCD spectra at 1698(−)/1688(+) attributed to the C2 7dbond;O stretch of thymine. The Mn^{2+}–DNA–protein complex also displays a strong positive peak in VCD at 1662 cm^{-1}, attributed to cytosine's C=O stretching accompanied by a shift and growth of the corresponding absorption at 1668 cm^{-1}. Because no similar changes were observed for the Mn^{2+}–DNA complexes even at high manganese concentrations[52] nor for the DNA–HMGB1/H1 complexes, it can be assumed that these features reflect the interactions induced by the presence of both Mn^{2+} ions and the proteins. These VCD features correspond to the changes in the mutual orientations of the groups, located in the minor groove rather than their interactions with some ligands. Hence, it is most likely that the presence of manganese affects the binding of HMGB1 to DNA, resulting in a different geometry of the minor groove and increasing optical activity of the corresponding carbonyls. This means that in the presence of manganese the proteins bend DNA stronger than without Mn^{2+} ions. Such behavior looks similar to the one observed earlier for the functional elements recruiting both HMGB-domain proteins and Mn^{2+} ions,[14] although the present DNA–HMGB1/H1 system is different.

Based on these results, it can be assumed that the extensive aggregation at higher r values observed in UV might be due to the ability of manganese ions to facilitate DNA compaction by HMGB1 and H1. As shown earlier[43] in a ternary DNA–protein complex, HMGB1 interacts with the bases and the positively charged histone H1 mostly interacts with phosphate groups—thus screening most of the DNA groups from the solution. This leads to the amplification of the interactions between the protein molecules, resulting in the increasing number of associations of the complexes, which were observed as ψ spectra. At the same time, at smaller r values (Figure 3) it is not very typical for the complexes and suggests an increase in structural order of the system accompanied by structural reorganization of the complexes after the addition of the manganese ions similar to those observed earlier for HMGB1–(A+B)/DNA complexes, which were also characterized by the high level of DNA compaction.[36,68] This process is illustrated in Figure 3, where the ellipticity of DNA at 280 nm (θ_{280}) is plotted against the protein to DNA ratio r. This diagram shows two r intervals of high negative ECD of DNA in the presence of Mn^{2+} instead of only one region as for the complexes with low or no Mn^{2+}. Besides the possibility of specific Mn^{2+}–protein interactions mentioned above, it is also possible that addition of the Mn^{2+} ions leads to electrostatic screening of the negatively charged acidic protein tail by the counterion layer. At small r when there are not enough H1 molecules in solution yet to screen negative charges of the molecules, this can result in increased affinity of the HMGB1 to the DNA and in weaker interactions between the HMGB1 and H1 molecules. The negative charge of the DNA sugar–phosphate backbone is also screened and DNA becomes more flexible, which makes the double helix more "attractive" for the proteins. Therefore, the VCD increase at low manganese concentrations can be attributed to the increase of the protein fraction actually bound to DNA and as a result more prominent structural changes of the double helix. The possibility of Mn^{2+} interacting with negatively charged groups of the protein was confirmed by our spectroscopic data and earlier crystallographic studies.[10,11] These experiments demonstrate that Mn^{2+} ions can readily coordinate with the aspartic and glutamic acid residues. The acidic tail of HMGB1 consists of these two particular amino acids, making it a likely target for the counterions. Hence, there is a possibility for the ions to affect the DNA-binding properties of the HMGB1 protein by interacting with its acidic tail and polar groups within the DNA-binding domain as well as with positively charged groups within the histone molecule.

Thus, the most significant influence on the protein DNA interaction caused by manganese ions occurs at low protein concentrations. This observation may be important for understanding the functioning of those biological systems in which the HMGB1/2 proteins participate in the functioning of other nuclear factors in quantities not sufficient to expect architectural function. For example, it was reported earlier that HMGB1/2 proteins in very low concentrations enhance the cleavage of DNA by RAG1/RAG2 proteins *in vitro* and *in vivo*.[13–16] The remarkable result of those experiments was the fact that HMGB1/2 enhanced the cleavage of the DNA hairpin structures at their tips, protecting the other sites from the enzyme attack and the essential cofactors of the reaction were divalent metal ions, Mn^{2+} in particular. The mechanism of such activity remains uncertain because the HMGB proteins do not possess even single-strand nicking activity. According to the experi-

ment with nucleosomes, this is also unlikely to be a result of the distortion induced by the HMGB1 on DNA.[73] Moreover, it was shown that during the later stages of V(D)J recombination events, HMGB1/2 as well as the recombinant proteins containing only HMGB domains enhance *ligation* activity of the double-strand breaks.[74] Taking into account the ability of the DNA-binding motif to recognize distortions on DNA and actually perform this function at several other stages of the recombination,[75] one could expect similar effects as a result of binding to the hairpin tip region. However, our results suggest that in the presence of manganese ions the mode of protein–DNA interaction can also change and possibly lead to preferential and enhanced binding to the sites on the DNA, which are not a usual target for the HMG–Box proteins.

Financial support is gratefully acknowledged from the Natural Sciences and Engineering Research Council of Canada (H. Wieser), Alberta Heritage Foundation for Medical Research (AHFMR) (V. Andrushchenko) and the Russian Foundation for Basic Research (A. M. Polyanichko, E. V. Chikhirzhina, and V. I. Vorob'ev; grants 04-04-49429 and 05-04-49217), the Federal Agency of Science and Innovation (02.445.11.7338), Program "Leading Scientific Schools of Russia" (9396.2006.4). Part of this work was performed during the tenure of an NSERC-NATO Science Fellowship and The Government of St. Petersburg (PD06-1.4-55). (A. M. Polyanichko). The authors also express their special gratitude to the Department of Chemistry at the University of Calgary for providing the instrumentation for UV and ECD spectroscopy.

REFERENCES

1. Silva, J. J. R. F. D.; Williams, R. J. P. The Biological Chemistry of the Elements; Clarendon Press: Oxford, 1991.
2. Glusker, J. R. Adv Protein Chem 1991, 42, 1–73.
3. Glusker, J. R.; Katz, A. K.; Bock, C. W. Rigaku J 1999, 16, 8–17.
4. Sigel, S.; Sigel, H., Eds. Metal Ions in Biological Systems: Manganese and Its Role in Biological Processes; Marcel Dekker: New York, Basel, 2000; Vol 37.
5. Patil, S. D.; Rhodes, D. G. Nucleic Acids Res 2000, 28, 2439–2445.
6. Feldman, A. R.; Sen, D. J Mol Biol 2001, 313, 283–294.
7. Noble, C. G.; Maxwell, A. J Mol Biol 2002, 318, 361–371.
8. Hays, H.; Berdis, A. J. Biochemistry 2002, 41, 4771–4778.
9. Oubrahim, H.; Chock, P. B.; Stadtman, E. R. J Biol Chem 2002, 277, 20135–20138.
10. Yamagata, A.; Kakuta, Y.; Masui, R.; Fukuyama, K. Proc Natl Acad Sci USA 2002, 99, 5908–5912.
11. Hadden, J. M.; Declais, A.-C.; Phillips, S. E. V.; Lilley, M. J. EMBO J 2002, 21, 3505–3515.
12. Bustin, M. Trends Biochem Sci 2001, 26, 152–153.
13. Santagata, S.; Aidinis, V.; Spanopoulou, E. J Biol Chem 1998, 273, 16325–16331.
14. Shockett, P. E.; Schatz, D. G. Mol Cell Biol 1999, 19, 4159–4166.
15. Mundy, C. L.; Patenge, N.; Matthews, A. G. W.; Oettinger, M. A. Mol Cell Biol 2002, 22, 69–77.
16. Swanson, P. C. Mol Cell Biol 2002, 22, 1340–1351.
17. Bustin, M.; Reeves, R. Prog Nucleic Acid Res Mol Biol 1996, 54, 35–100.
18. Bustin, M. Mol Cell Biol 1999, 19, 5237–5246.
19. Webb, M.; Thomas, J. O. J Mol Biol 1999, 294, 373–387.
20. Ohno, T.; Umeda, S.; Hamasaki, N.; Kang, D. Biochem Biophys Res Commun 2000, 271, 492–498.
21. Bianchi, M. E.; Beltrame, M.; Paonessa, G. Science 1989, 243, 1056–1059.
22. Gariglio, M.; Ying, G. G.; Hertel, L.; Gaboli, M.; Clerc, R. G.; Landolfo, S. Exp Cell Res 1997, 236, 472–481.
23. Bianchi, M. E.; Beltrame, M. Am J Hum Genet 1998, 63, 1573–1577.
24. Segall, A. M.; Goodman, S. D.; Nash, H. A. EMBO J 1994, 13, 4536–4548.
25. Thomas, J. O. Biochem Soc Trans 2001, 29, 395–401.
26. Zlatanova, J.; van Holde, K. Bioessays 1998, 20, 584–588.
27. Kohlstaedt, L. A.; Sung, E. C.; Fujishige, A.; Cole, R. D. J Biol Chem 1987, 262, 524–526.
28. Kohlstaedt, L. A.; Cole, R. D. Biochemistry 1994, 33, 570–575.
29. Baxevanis, A. D.; Landsman, D. Nucleic Acids Res 1995, 23, 1604–1613.
30. Copenhaver, G. P.; Putnam, C. D.; Denton, M. L.; Pikaard, C. S. Nucleic Acids Res 1994, 22, 2651–2657.
31. Jantzen, H. M.; Admon, A.; Bell, S. P.; Tjian, R. Nature 1990, 344, 830–836.
32. Lu, W.; Peterson, R.; Dasgupta, A.; Scovell, W. M. J Biol Chem 2000, 275, 35006–35012.
33. Sutrias-Grau, M.; Bianchi, M. E.; Bernues, J. J Biol Chem 1999, 274, 1628–1634.
34. Lichota, J.; Grasser, K. D. Biol Chem 2003, 384, 1019–1027.
35. Zhang, S. B.; Huang, J.; Zhao, H.; Zhang, Y.; Hou, C. H.; Cheng, X. D.; Jiang, C.; Li, M. Q.; Hu, J.; Qian, R. L. Cell Res 2003, 13, 351–359.
36. Polyanichko, A. M.; Chikhirzhina, E. V.; Skvortsov, A. N.; Kostyleva, E. I.; Colson, P.; Houssier, C.; Vorob'ev, V. I. J Biomol Struct Dyn 2002, 19, 1053–1062.
37. Diez-Caballero, T.; Aviles, F. X.; Albert, A. Nucleic Acids Res 1981, 9, 1383–1393.
38. Zlatanova, J.; Yaneva, J. DNA Cell Biol 1991, 10, 239–248.
39. Widom, J. Annu Rev Biophys Biomol Struct 1998, 27, 285–327.
40. Travers, A. Trends Biochem Sci 1999, 24, 4–7.

41. Jordan, C. F.; Lerman, L. S.; Venable, J. H. Nat New Biol 1972, 236, 67–70.
42. Tinoco, I., Jr.; Mickols, W.; Maestre, M. F.; Bustamante, C. Annu Rev Biophys Biophys Chem 1987, 16, 319–349.
43. Polyanichko, A. M.; Wieser, H. Biopolymers 2005, 78, 329–339.
44. Polavarapu, P. L.; Zhao, C. J Anal Chem 2000, 366, 727–734.
45. Keiderling, T. A. Curr Opin Chem Biol 2002, 6, 682–688.
46. Andrushchenko, V.; Tsankov, D.; Wieser, H. J Mol Struct 2003, 661–662, 541–560.
47. Oliver, D.; Sommer, K. R.; Panyim, S.; Spiker, S.; Chalkley, R. Biochem J 1972, 129, 49–353.
48. Johns, E. W. The HMG Chromosomal Proteins; Academic Press: London 1982; 43–45, 59–60.
49. Laemmli, U. K. Nature 1970, 227, 680–685.
50. Tsankov, D.; Eggimann, T.; Wieser, H. Appl Spectrosc Rev 1995, 49, 132–138.
51. Galactic Industries Corporation. Labcalc, C2.24; Salem, NH, 1992.
52. Polyanichko, A. M.; Andrushchenko, V. V.; Chikhirzhina, E. V.; Vorob'ev, V. I.; Wieser, H. Nucleic Acids Res 2004, 32, 989–996.
53. Tsuboi, M. Appl Spectrosc Rev 1969, 3, 45–90.
54. Tsuboi, M. In Basic Principles in Nucleic Acid Chemistry; Ts'o, P. O. P., Ed.; Academic Press: New York, 1974; pp 399–452.
55. Taillandier, E.; Liquier, J.; Taboury, J. A. In Advances in Infrared and Raman Spectroscopy; Clark, R. J. H., Hester, R. E., Eds.; Wiley Heyden: New York, 1985; Vol 12, pp 65–114.
56. Tajmir-Riahi, H. A.; Naoui, M.; Ahmad, R. Biopolymers 1993, 33, 1819–1827.
57. Alex, S.; Dupuis, P. Inorg Chim Acta 1989, 157, 271–281.
58. Annamalai, A.; Keiderling, T. A. J Am Chem Soc 1987, 109, 3125–3132.
59. Wang, L.; Keiderling, T. A. Biochemistry 1992, 31, 10265–10271.
60. Wang, L.; Yang, L.; Keiderling, T.A. Biophys J 1994, 67, 2460–2467.
61. Diem, M. Spectroscopy, 1995, 10, 38–43.
62. Keiderling, T. A. In Circular Dichroism and the Conformational Analysis of Biomolecules; Fasman, G. D., Ed.; Plenum Press: New York, 1996; pp 555–597.
63. Andrushchenko, V.; Leonenko, Z.; Cramb, D.; van de Sande, H.; Wieser, H. Biopolymers 2001, 61, 243–260.
64. Bour, P.; Andrushchenko, V.; Kabelac, M.; Maharaj, V.; Wieser, H. J Phys Chem B 2005, 109, 20579–20587.
65. Andrushchenko, V.; van de Sande, J.; Wieser, H. Biopolymers 2003, 69, 529–545.
66. Baumruk, V.; Keiderling, T. A. J Am Chem Soc 1993, 115, 6939–6942.
67. Barth, A. Prog Biophys Mol Biol 2000, 74, 141–173.
68. Chikhirzhina, E. V.; Polyanichko, A. M.; Skvortsov, A. N.; Kostyleva, E. I.; Houssier, C.; Vorob'ev, V. I. Mol Biol 2002, 36, 525–531.
69. Chikhirzhina, E. V.; Kostyleva, E. I.; Ramm, E. I.; Vorob'ev, V. I. Tsitologiia 1998, 40, 883–888.
70. Tinoco, I., Jr.; Mickols, W.; Maestre, M. F.; Bustamante, C. Ann Rev Biophys Biophys Chem 1987, 16, 319–349.
71. Lee, K.-B.; Thomas, J. O. J Mol Biol 2000, 304, 135–149.
72. Polyanichko, A. M. Ph.D. thesis, St. Petersburg State University, 2003.
73. Golding, A.; Chandler, S.; Ballestar, E.; Wolffe, A. P.; Schlissel, M. S. EMBO J 1999, 18, 3712–3723.
74. Nagaki, S.; Yamamoto, M.; Yumoto, Y.; Shirakawa, H.; Yoshida, M.; Teraoka, H. Biochem Biophys Res Commun 1998, 246, 137–141.
75. Aidinis, V.; Bonaldi, T.; Beltrame, M.; Santagata, S.; Bianchi, M. E.; Spanopoulou, E. Mol Cell Biol 1999, 19, 6532–6542.

Reviewing Editor: Sarah Woodson